




Comparative Study of Surface Roughness in Upskin and Downskin Regions of Conformal Cooling Channel Sections Fabricated with AlSi10Mg, Ti64, 316L in AM-LPBF

Cemal İrfan Çalışkan¹ 

Article Info

Received: 06 Mar 2025

Accepted: 13 Apr 2025

Published: 30 Jun 2025

Research Article

Abstract – Conformal cooling channel (CCC), used in many industries such as aviation, molding, biomedical, and robotics, refers to functional fluid channels that provide mass or energy transfer. CCC, which can be produced in limited forms where liquid flow cannot be fully achieved in traditional production technologies, is among the areas where additive manufacturing (AM) offers design freedom. However, in design-integrated CCC productions, sagging and deformation in the pipe section caused by the AM production process and design parameters can cause a decrease in the performance expected from the CCC and cause unpredictable flow problems. The producible CCC section from research constitutes the scope of this study. In this study, the production of cylindrical test specimens with eleven channel cross-sections between 0,4 mm and 9 mm using laser powder bed fusion (LPBF) technology using AlSi10Mg, 316L, and Ti64 materials and the roughness measurements of the upskin and downskin regions and the scanning electron microscope (SEM) examination are comparatively discussed. Inconsistent results were obtained in the surface roughness measurements of the 0,4 mm and 0,5 mm diameter holes considered within the scope of the research due to the diameter being below the production limits. This research shows that surface roughness in the upskin parameter region is more acceptable in all material types. In the laboratory measurements obtained, it is seen that the downskin region surface roughness value in the holes produced with AlSi10Mg is higher than other materials, and it is lower in the holes produced with Ti64 than other materials.

Keywords – Additive manufacturing, laser powder bed fusion, AlSi10Mg, 316L, Ti64, conformal cooling channels

1. Introduction

AM is the formalized generic term for the technology popularly known as 3D Printing, also called rapid prototyping [1]. The term is used in various industries to describe rapidly creating a part representation before the final product or commercialization [2]. In other words, creating a physical part directly from digital model data has been widely used to describe technologies that develop prototypes. Nowadays, rapid prototyping technologies are not only used to create models. However, they were initially designed to expand the range of situations tested in the prototyping process. Still, with the advantages of certain materials, it is now possible to create finished products [3]. American Society for Testing and Materials International (ASTM) has defined additive manufacturing as combining materials in layers to produce objects from Computer Aided Design (CAD) model data [4]. While Additive Manufacturing (AM) has existed as a method of processing materials for over three decades, it is now emerging as an essential commercial manufacturing technology.

¹cemalirfancaliskan@gmail.com (Corresponding Author)

¹Department of Industrial Design, Faculty of Architecture, Istanbul Technical University, İstanbul, Türkiye

AM, which has been the focus of research since the 1980s, has created new design areas in many industrial areas with its new perspective. One of these innovative areas is the manufacturability of complex internal geometries, functional fluid channels [5]. Various studies on these functional flow channels [6] and complex internal geometries are encountered in areas such as electronic cooling [7], biomedical [8], heat exchangers [9], and molds [10,11].

Research on functional flow channels produced by AM and aimed at regulating cooling performance is referred to in the literature as conformal cooling channels (Figure 1). Various studies in the AM field show that Conformal Cooling Channel (CCC) [12] is a good solution to control thermal stresses, improve the quality of the final product, and reduce cycle time [13].

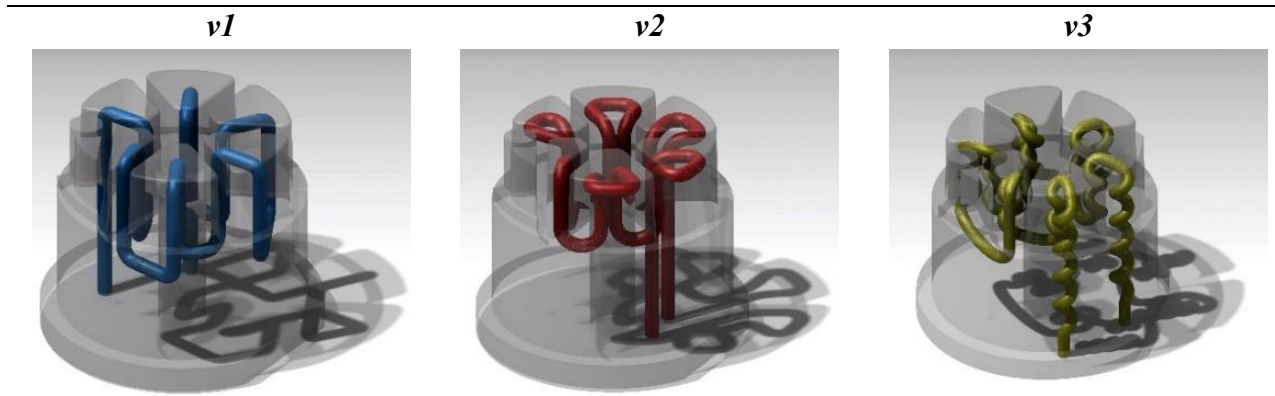


Figure1. Various CCC designs [14]

These systems have a promising future in replacing conventional cooling systems as they can provide more efficient cooling effects and contribute significantly to production quality [15] and efficiency [16]. Some studies indicate that the cycle time is shortened by 30% [17] and 40% in injection systems where CCC-applied molds are used [14]. Some studies on this subject report that production cycle time can be reduced by up to 70%, and shape deviations can be prevented [18]. The diameter of the Conformal Cooling (CC) channels and the ability to manufacture the channel cross-section [19] that does not obstruct the coolant flow play an essential role in cooling and production efficiency in molds and part quality [20]. Some research results show that CC channel-applied eco-friendly molds shorten the cooling time by 45% [21].

The different efficiency values obtained in the research are directly related to the mold size, CCC geometry diameter of this size, the manufacturability of the channel section, and the channel's inner surface roughness. The surface roughness factor is essential in evaluating the CCC channels' liquid pressure drop [22]. It is known that some post-processing, known as abrasive flow machining, is performed to eliminate the unpredictable and inhomogeneous surface roughness in the channel cross-section of 1 to 2 mm diameter channels produced with Laser Powder Bed Fusion (LPBF) [23].

There are not many studies in the literature about the channel cross-sectional form and upskin and downskin regions in the holes of CCC geometries, which are generally known to provide advantages such as increased production quality [24], increased production time [25], energy saving, and efficiency [26].

Our previous studies on channel geometries produced without support determined that some sagging or deformations occurred on the upper surface of the hole where the downskin parameter was effective [27]. In another study we conducted in this context, since the actual surface roughness of the upskin and downskin regions within the channel could not be determined in the channel cross-sections examined with imaging methods such as Computed Tomography (microCT) and Scanning Electron Microscope (SEM) [28], a comparative study was conducted on the surface roughness, which is known to be effective in flow quality in the upskin and downskin regions, with the method presented in this study. Since the probe measurement method of the roughness measuring devices requires the surface to be open from the top, each hole sample was produced in two pieces, and precise vertical surface roughness measurements were completed. Three

roughness values taken from each hole sample are shared comparatively in this research using AlSi10Mg, 316L, and Ti64 materials. In addition, SEM examination was included to show that the sagging effect, which is more intense in hole diameters smaller than 2 mm and where the downskin parameter is effective, is not very effective in larger diameters.

2. Materials

Considering the basic design criteria (Table 1), the LPBF technology manufacturer provided support-free production that can be carried out in channel sections between 0,5 mm and 8 mm.

Table 1. LPBF design parameters [29,30]

The ratio between the section and height of the object to be produced should not be more than 8:1	The outside-to-outside dimensions of the design should not be larger than the platform size	Alternative geometries should be used for sizes larger than 8mm, which are desired to be produced without support
The minimum hole diameter in the design should not be less than 0,5 mm	The maximum hole diameter to be produced without support should be 8mm	The minimum diameter for the cylinder geometry used in the design should not be less than 1 mm
Unsupported angles should not be less than 30-45 degrees. Angle evaluation varies depending on the material used.	Part dimensional tolerance: +, - 0,1 mm	The minimum producible wall thickness should not be less than 0,4mm

Therefore, the hole diameters determined in this research were preferred in this range (Figure 2). Hole test sample designs in the determined range were completed in the Catia V5 part design module, and the research continued with the production process.

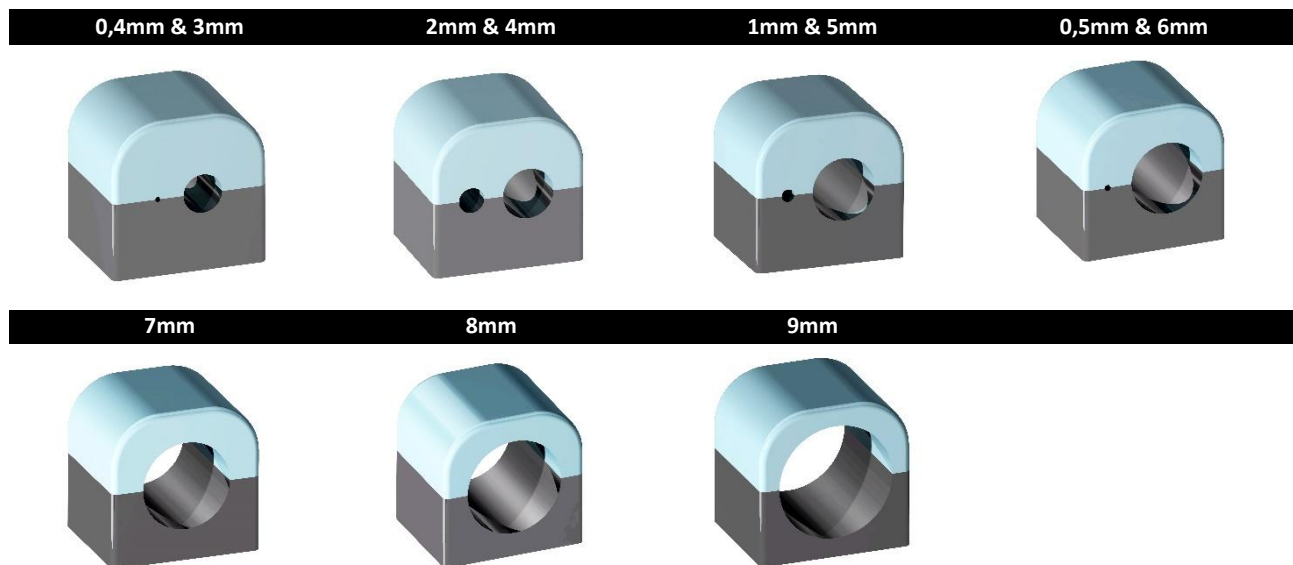


Figure 2. CAD images of the two-piece test samples designed with Catia V5 within the scope of the study

The hole test samples in Figure 2 were designed in two pieces to be able to measure from the bottom and top surfaces of the hole. In this context, some hole diameters were placed in the same sample due to their scale (0,4 mm & 3 mm), and surface roughness measurements were made with three repetitions for each diameter value.

The productions made within the scope of this research were carried out with EOS M290 using AlSi10Mg, 316L, and Ti64 materials. The prevalence of use in the sector was considered in the material selection. In this direction, AlSi10Mg, which is used intensively in electronic cooling, thermal fields, and AM productions, stainless steel 316L used in CCC integrated molding applications, and Ti64, which is a biocompatible material within the scope of CCC's use in the biomedical field, were preferred.

LPBF production technology uses a special parameter set called upskin when the surface faces upwards and downskin when it faces downwards in some sensitive areas of internal geometries. The region and scanning strategy where the upskin and downskin parameters used in the hole samples produced in this study are visualized in Figure 3.

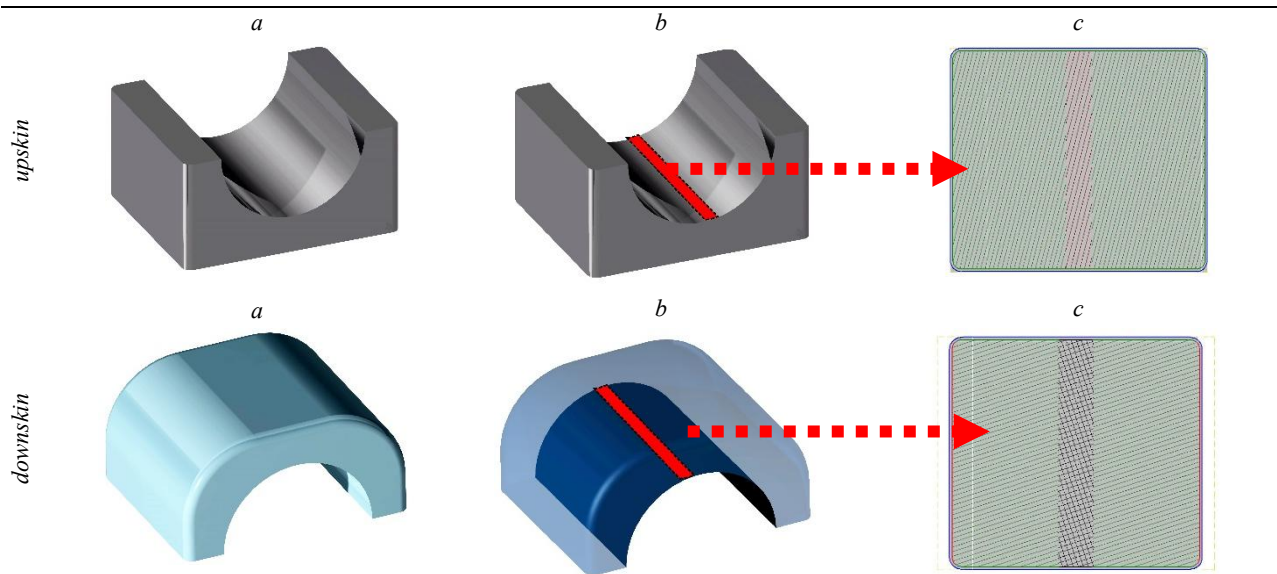


Figure 3. a. Test sample lower and upper CAD, b. upskin & downskin scanning area, c. upskin & downskin scanning area in the EOS print software

The following energy formula (2.1), expressing the balance between the parameters, is used in the research on the process parameter changes. In parameter optimization research to solve the sagging problem of the downskin region, these parameters can be used in production by equalizing the value of the formula [31].

$$E = \frac{P}{vht} \quad (2.1)$$

In this formula, E represents energy, P represents laser power, v represents laser scanning speed, h represents scanning distance, and t represents layer thickness. Upskin and downskin default parameter sets were used in sample production, with three different materials used within the scope of this study (Table 2).

Table 2. EOS upskin and downskin parameters of AlSi10Mg, 316L, and Ti64 materials

	parameters	upskin	downskin
AlSi10Mg	hatchdistance:	0,21 mm	0,21 mm
	scanning speed:	1000 mm/s	1150 mm/s
	laser power:	360 W	340 W
	thickness:	0,09 mm	0,06 mm
	scanning strategy:	X-Y-Alternating	X-Y
316L	hatchdistance:	0,09 mm	0,1 mm
	scanning speed:	800 mm/s	1000 mm/s
	laser power:	135 W	80 W
	thickness:	0,04 mm	0,06 mm
	scanning strategy:	X-Y-Alternating	X-Y-Alternating
Ti64	hatchdistance:	0,04 mm	0,1 mm
	scanning speed:	1200 mm/s	1000 mm/s
	laser power:	280 W	120 W
	thickness:	0,09 mm	0,06 mm
	scanning strategy:	X-Y	X-Y

3. Methods

3.1. AM Fabrication

Within the scope of the study, the LPBF production phase was started after the CAD design phase. The chemical composition of the materials used in production, AlSi10Mg, 316L, and Ti64, is shared in Table 3.

Table 3. Chemical composition of AlSi10Mg (DIN EN 1706) [32], 316L (ASTM F138) [33] and Ti64 (ASTM F1472 and ASTM F2924) [34]

	<i>Al</i>	<i>Si</i>	<i>Fe</i>	<i>Cu</i>	<i>Mn</i>	<i>Mg</i>	
AlSi10Mg	balance	% 9,0-11	% 0,55	% 0,05	% 0,45	% 0,25-0,45	<i>Generic particle size distribution</i> 25 - 70 μm
	<i>Ni</i>	<i>Zn</i>	<i>Pb</i>	<i>Sn</i>	<i>Ti</i>		
	% 0,05	% 0,10	% 0,05	% 0,05	% 0,15		
316L	<i>Fe</i>	<i>Cr</i>	<i>Ni</i>	<i>Mo</i>	<i>C</i>	<i>N</i>	20 – 65 μm
	balance	%17-19	%13-15	%2,25-3	%0,03	%0,10	
	<i>Al</i>	<i>V</i>	<i>O</i>	<i>N</i>	<i>C</i>	<i>H</i>	
Ti64	% 5,50-6,75	%3,50-4,50	%0,20	%0,05	%0,08	%0,015	20 – 80 μm
	<i>Fe</i>	<i>Y</i>	<i>Ti</i>	<i>other, each</i>	<i>other, total</i>		
	%0,30	%0,005	balance	%0,10	%0,40		

During the production phase, the CAD data of the hole sample set exported in STL format was placed in the magics software, and the supports were determined (Figure 4a). In order to use the upskin and downskin parameters, the upper and lower surfaces of the holes were positioned in the orientation of the test samples produced in two pieces, preserving their positions. The production file, which was layer-controlled with the EOS print software, was sent to the production system, and the process was started. The images of the test samples coming out of production are shared in Figures 4b and c.

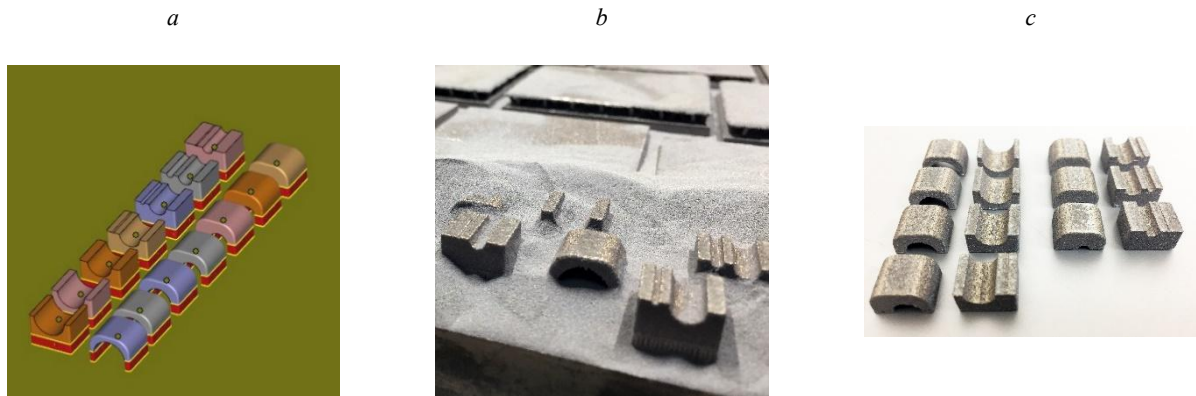


Figure 4. a. Orientation and support of test samples in Magics software, b. LPBF production of test samples, c. Completed test samples

3.2. Laboratory Studies

After the production, the upskin and downskin regions of the 1 mm and 4 mm diameter samples were imaged with the SEM device without any post-processing other than removing the supports from the parts (Figure 5).

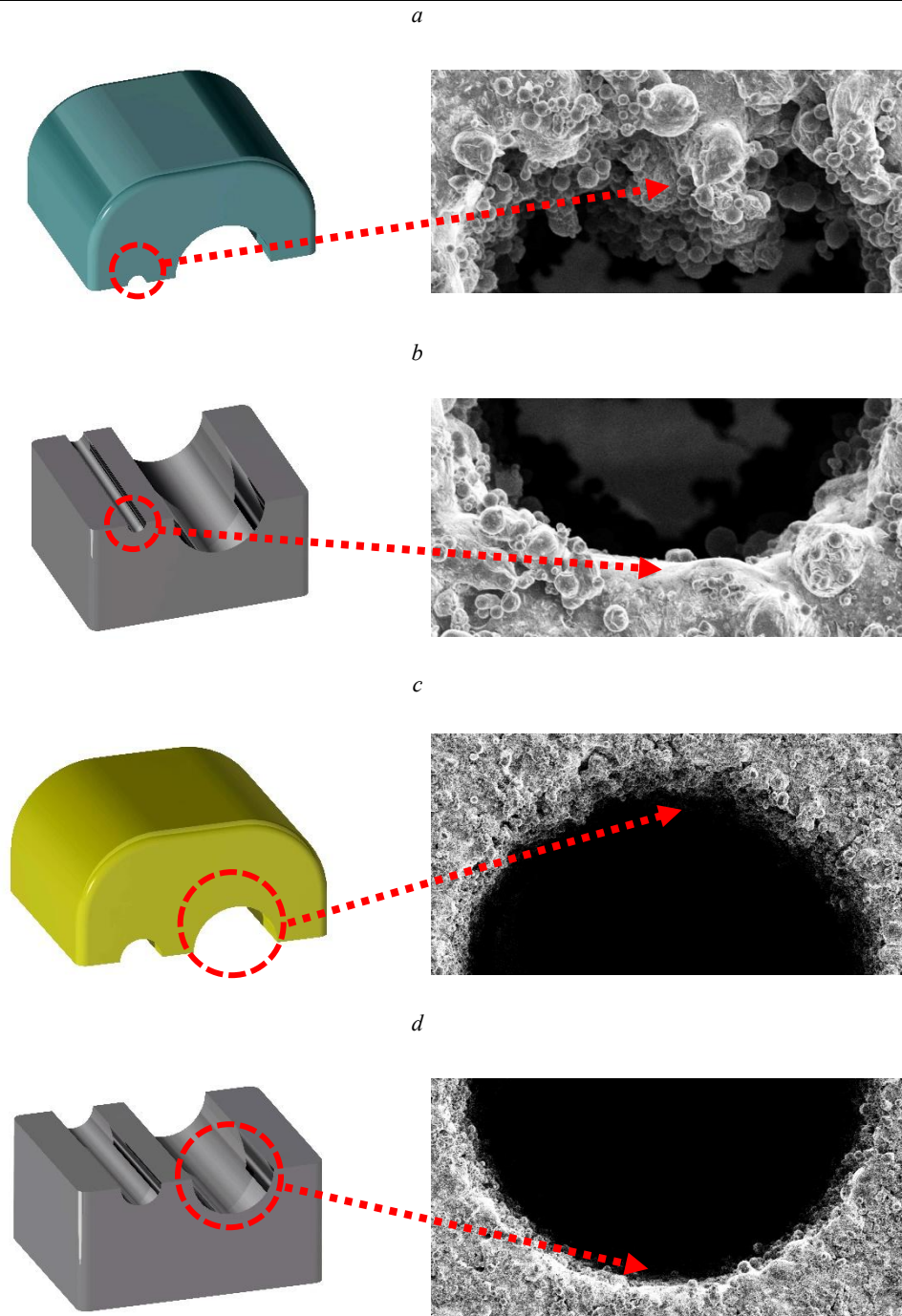


Figure 5. Sem images and CADs. a. 1 mm diameter CCC section in the downskin region, b. 1 mm upskin region, c. 4 mm downskin region, d. 4 mm upskin region

In SEM images, which support the data obtained in previous studies in this field [19], the sagging problem in the downskin region (Figure 5a) is seen, especially in low diameters. According to the SEM examination, the hole cross-section form can be produced with higher quality in large diameters. It is known that SEM examinations give results comparable to CAD in in-hole measurements. However, separately measuring the surface roughness values in the upskin and downskin regions is essential for performing functional channel geometries. In this context, the data obtained from surface roughness measurements made with Mitutoyo SJ-500 will be included in the results section as the top and bottom surfaces. The roughness measurements (Figure 6), the average of three measurements taken linearly in the upskin and downskin regions according to the sample size, were taken.

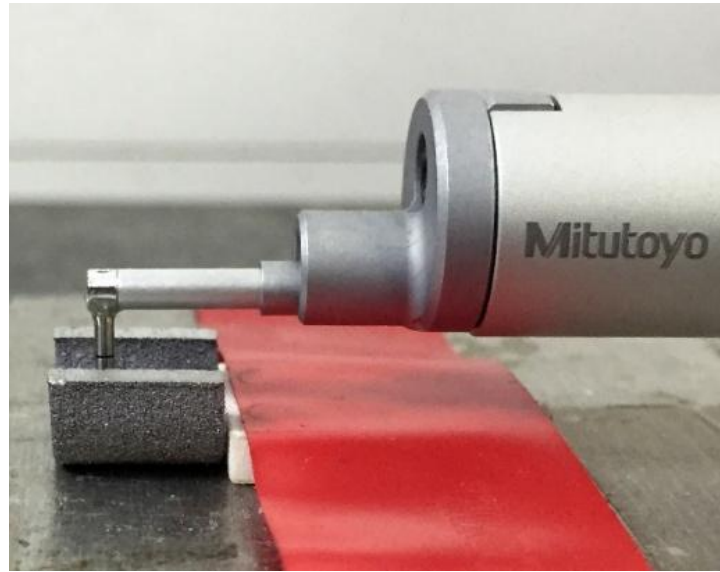


Figure 6. Mitutoyo SJ-500 surface roughness measurement

4. Results and Discussion

The hole diameter range determined within the scope of the research is between 0,4 mm and 9 mm. Accordingly, the test samples produced include hole diameters of 0,4 and 0,5 mm. However, in making small-diameter LPBF circular forms, the distortion of the hole geometry due to sagging and its transformation into an elliptical form led to inconsistent results in surface roughness measurements. Considering the requirement that hole diameters be greater than 0,5 mm in the design criteria shared by the LPBF manufacturer, it can be said that it is normal to obtain inconsistent surface roughness values from hole diameters in this range. In addition, it is considered acceptable that using circular probes in surface roughness measurement devices gives inconsistent results in measuring small-diameter circular forms that are deteriorated by sagging.

The data of surface roughness measurements made in the upskin parameter regions of hole test samples produced with AlSi10Mg, 316L, and Ti64 materials are shared in Figure 7.

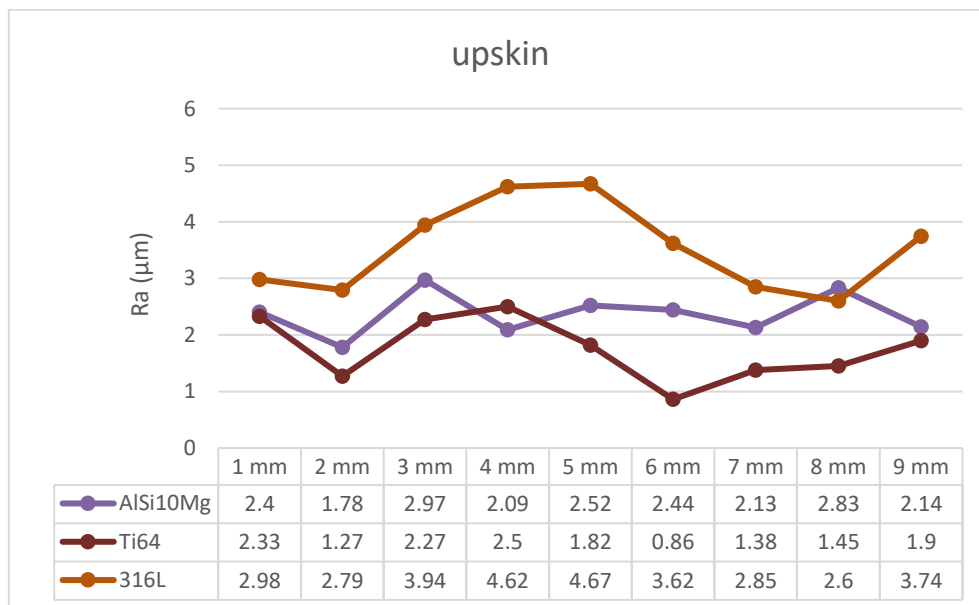


Figure 7. Surface roughness values in the upskin parameter region of hole sections with 1-9 mm diameters produced with AlSi10Mg, 316L, and Ti64 materials

According to Figure 7, the surface roughness values in the upskin region of the holes produced with 316L are higher than those produced with AlSi10Mg and Ti64 in all holes. It can be stated that the upskin surface roughness values of the holes produced with AlSi10Mg are at an average level compared to the other two materials. In the measurements made in the upskin parameter region, it is seen that the lowest roughness values are obtained with Ti64 material. In the evaluation of Figure 7, it can be stated that the 316L and Ti64 upskin surface roughness graphs exhibit a similar change between the holes, although they are in different value ranges. However, it is seen that the graph obtained from the measurement of test samples produced with AlSi10Mg is quite different from the graphs of the other two materials, and that the surface roughness values between the holes give very close results in this material. The results obtained with 316L and Ti64 materials show that while the roughness values between the holes give close values at 2 and 6 mm, this distance widens considerably at 3, 4, 5, 8, and 9 mm (Figure 7).

This situation is thought to be directly related to the technology manufacturer's development process and material properties of the upskin parameter set.

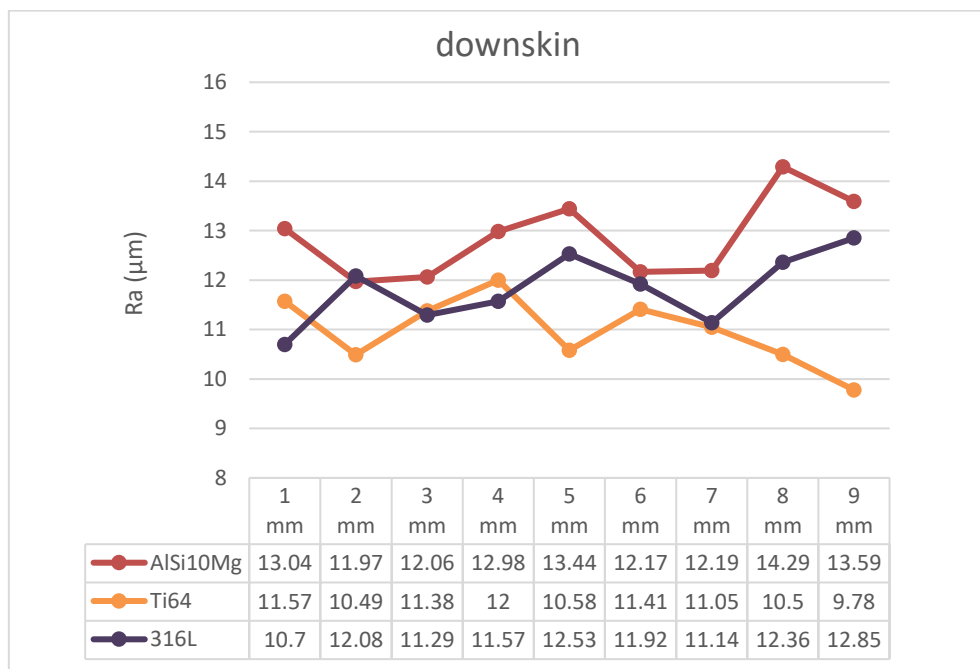


Figure 8. Surface roughness values in the downskin (where the sagging effect is seen) parameter region of hole sections with 1-9 mm diameters produced with AlSi10Mg, 316L, and Ti64 materials.

The surface roughness values measured from the downskin region of the test samples with hole diameters of 1-9 mm produced with LPBF are shared in Figure 8. According to Figure 8, the roughness value of the downskin region in the holes produced with AlSi10Mg is higher than in other materials. According to this graphic data, sagging will be more intense in the upper region of the holes produced with AlSi10Mg. It is seen that the surface roughness value of the downskin region in the holes produced with Ti64 is generally lower than in other materials. It can be stated that the roughness values taken from the downskin surface parameter region of the holes produced with 316L material are generally higher than Ti64 and lower than AlSi10Mg. However, it can be stated that this situation is out of generalization in some hole measurements, such as 1 mm and 4 mm.



Figure 9. Surface roughness values from the upskin regions with each hole comparison

If we consider the surface roughness values from the upskin regions with each hole comparison (Figure 9) in terms of the three materials within the scope of this research, the following can be stated:

Upskin region surface roughness measurements represent the values taken from the lower arc ce. Figure 9 shows that the surface roughness values obtained from the holes produced with 316L material are 2,6 – 4,67 μm . In this value range, which represents the average of the surface roughness measurements made in three repetitions for each hole, the lowest value of 2,6 μm is seen in the 8 mm hole; the highest value of 4,67 μm is seen in the 5 mm hole. In general, it is seen that the 316L material gives the highest roughness values when compared with the other two materials. The hole is cylindrical.

According to the surface roughness measurements taken from the upskin parameter region of the productions made with Ti64, it is seen that all measurement values are in the range of 0,86 – 2,5 μm . It can be stated that this range is the lowest surface roughness value range for the three materials for upskin measurements. However, in the measurements taken only over 4 mm, it is seen that the roughness value of Ti64, which is 2,5 μm , is 2,09 μm in AlSi10Mg.

According to Figure 9, it can be stated that the upskin measurement results made with AlSi10Mg are in the range of 1,78 – 2,97 μm . It is seen that the lowest roughness value of 1,78 μm belongs to the 2 mm hole upskin measurement; the highest roughness value of 2,97 μm belongs to the 3 mm hole upskin measurement. Although it is an unexpected situation that two extreme values were taken in the roughness measurement of two very close hole diameters, considering that both values and the surface roughness values of all holes produced with AlSi10Mg are very close to each other, it is thought that this situation may be due to unforeseen layer shifting during the production process.

In the general evaluation to be made, it is seen that there is a difference of 2,07 μm between the highest and lowest surface roughness values obtained from holes produced with 316L material; this difference is 1,64 μm in surface roughness measurements taken from the upskin parameter region of productions made with Ti64; and 1,19 μm in AlSi10Mg. In light of this information, when all materials and hole diameters are compared, it is seen that the upskin parameter gives the least variable values in terms of surface roughness obtained in hole productions made with AlSi10Mg material; 316L has the most variable value range. It can be stated that this situation is due to the parameter set development process of the technology manufacturer and the material difference. However, it is thought that it would be correct to investigate the subject with different analysis and test methods in future studies.

Suppose we consider the surface roughness values from the downskin regions with each hole comparison (Figure 10) in terms of the three materials within the scope of this research. The following can be stated: The average of three surface roughness values measured from the downskin parameter region of hole test samples fabricated using AlSi10Mg, 316L, and Ti64 materials is shared graphically for each hole in Figure 10.

According to Figure 10, the surface roughness values measured from the downskin region of the productions made using 316L material are 10,70 – 12,85 μm . The 10,70 μm value is the surface roughness value measured from the downskin region of the 1 mm diameter hole, and the 12,85 μm surface roughness value is the surface roughness value measured from the 9 mm diameter. In the test sample productions made using Ti64 material, it is seen that the surface roughness values measured from the downskin region are in the range of 9,78 - 12 μm . Figure 10 shows that the 9,78 μm value belongs to the 9 mm hole, and the 12 μm measurement belongs to the 4 mm hole. It is seen that the maximum and minimum measurement values of AlSi10Mg downskin are in the range of 11,97 – 14,29 μm . It can be stated that the lowest roughness value of 11,97 μm belongs to the 2 mm hole, and the highest value of 14,29 μm belongs to the 8 mm hole (Figure 10).

Considering that the differences between the maximum and minimum measurements in downskin measurements are 2,15 μm in 316L material, 2,22 μm in Ti64 material, and 2,32 μm in AlSi10Mg, it is seen that the measurement range in all materials develops at similar rates around 2 μm .

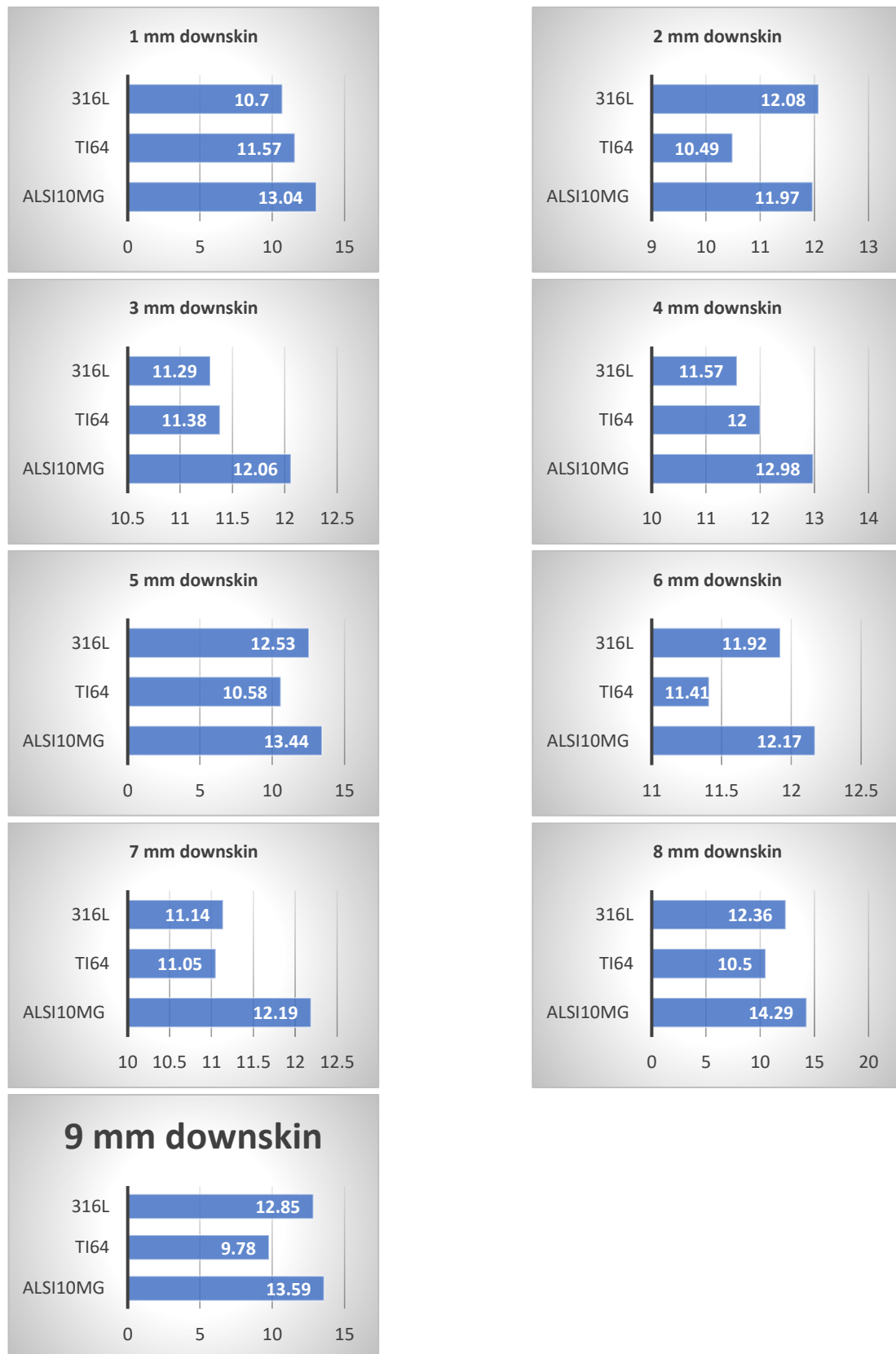


Figure 10. Surface roughness values from the downskin regions with each hole comparison

5. Conclusion

Within the scope of this study, upskin and downskin surface roughness measurements were made on hole test samples produced in AM-LPBF using AlSi10Mg, 316L, and Ti64 materials. The results obtained were compared in the context of the parameter region where the measurement was made, the three materials used in production, and the different holes. In this context, the following can be stated in light of the obtained data:

- i. The measurements made within this research's scope show significant differences between the surface roughness values measured from the upskin and downskin parameter regions. In the measurements made in this context, it is seen that the surface roughness values measured from the upskin region, regardless of the material difference, are in the range of 0,86 – 4,67 μm , while the measurements taken from the downskin region are in the range of 9,78 – 14,29 μm . In this context, future research may focus on the downskin region for better channel flow efficiency.
- ii. In the surface roughness measurements of the 0,4 mm and 0,5 mm diameter holes considered within the scope of the research, inconsistent results were obtained due to the standard probe measurement method of the roughness measuring devices and the hole diameter being smaller than the measuring device probe. Considering that the LPBF manufacturer's hole diameters must have a manufacturability range greater than 0.5 mm, 1 mm and above should be preferred in CCC designs.
- iii. It can be said that the surface roughness in the upskin parameter region is more acceptable in terms of maintaining the flow pressure in the channels; however, it is thought that the measurements in the downskin parameter region in the upper hole region will be effective in the channel pressure drop with higher surface roughness values. In future research and analysis studies, the surface roughness in the upskin and downskin regions should be considered within the scope of the flow pressure performance of these two regions and examined in more detail.
- iv. The surface roughness values in the upskin region of the holes produced with 316L are higher than those produced with AlSi10Mg and Ti64 in all hole diameters. It can be said that the upskin surface roughness values of the holes produced with AlSi10Mg are at an average level compared to the other two materials. In the measurements made in the upskin parameter region, it is seen that the lowest roughness values are obtained with Ti64 material. Considering that the surface roughness measurements in the upskin region are lower than the measurements in the downskin region, it is thought that this low roughness obtained with Ti64 will not provide significant advantages in terms of flow in the CC channels. Still, the subject should be investigated with analysis studies in the new research.
- v. The roughness value of the downskin region in the holes produced with AlSi10Mg is observed to be higher than that of other materials. In this context, it can be stated that sagging will be more intense in the upper region of the holes produced with AlSi10Mg. In light of this information, it can be noted that if AlSi10Mg is used in CCC applications, the flow performance will be lower than the other two materials considered in this research.
- vi. In holes produced with Ti64, it is seen that the surface roughness value of the downskin region is lower than in other materials. Therefore, in the evaluation to be made within the scope of flow pressure in CCC applications where this material is used, it is thought that the efficiency will be better than the other two materials.
- vii. The surface roughness values measured from the downskin surface parameter region of the holes produced with 316L material are observed to be higher than Ti64 and lower than AlSi10Mg. It can be stated that 316L material is more efficient than AlSi10Mg and acceptable compared to Ti64 for CCC applications.

Table 4. NOMENCLATURE

AM	Additive manufacturing
LPBF	Laser powder bed fusion
DMLS	Direct Metal Laser Sintering (LPBF Production System by EOS)
CCC	Conformal Cooling Channel
ASTM	American Society for Testing and Materials International
CAD	Computer-Aided Design
CT	Computed Tomography
SEM	Scanning Electron Microscope
CC	Conformal Cooling
Ra	Surface Roughness
E	Energy
P	Laser Power
v	Laser Scanning Speed
h	Scanning Distance
t	Layer Thickness

Author Contributions

The author read and approved the final version of the paper.

Conflict of Interest

The author declares no conflict of interest.

Ethical Review and Approval

No approval from the Board of Ethics is required.

References

- [1] I. Gibson, D. Rosen, B. Stucker, M. Khorasani, D. Rosen, B. Stucker, M. Khorasani. Additive Manufacturing Technologies, 17 (2021).
- [2] C. İ. Çalışkan, Ü. Arpacioğlu. *Additive manufacturing on the façade: functional use of direct metal laser sintering hatch distance process parameters in building envelope*, Rapid Prototyping Journal 28 (9) (2022) 1808–1820.
- [3] K. V Wong, A. Hernandez. *A review of additive manufacturing*, International Scholarly Research Notices 2012 (1) (2012) 208760.
- [4] W. E. Frazier. *Metal additive manufacturing: a review*, Journal of Materials Engineering and Performance 23 (2014) 1917–1928.
- [5] C. Zhang, S. Wang, J. Li, Y. Zhu, T. Peng, H. Yang. *Additive manufacturing of products with functional fluid channels: A review*, Additive Manufacturing 36 (2020) 101490.
- [6] B. B. Kanbur, Y. Zhou, S. Shen, K. H. Wong, C. Chen, A. Shocket, F. Duan. *Metal additive manufacturing of plastic injection molds with conformal cooling channels*, Polymers 14 (3) (2022) 424.

- [7] Y. Li, S. Roux, C. Castelain, Y. Fan, L. Luo. *Design and optimization of heat sinks for the liquid cooling of electronics with multiple heat sources: A literature review*, Energies 16 (22) (2023) 7468.
- [8] V. K. Lee, D. Y. Kim, H. Ngo, Y. Lee, L. Seo, S.-S. Yoo, P. A. Vincent, G. Dai. *Creating perfused functional vascular channels using 3D bio-printing technology*, Biomaterials 35 (28) (2014) 8092–8102.
- [9] S. A. Niknam, M. Mortazavi, D. Li. *Additively manufactured heat exchangers: A review on opportunities and challenges*, The International Journal of Advanced Manufacturing Technology 112 (3) (2021) 601–618.
- [10] S. Feng, A. M. Kamat, Y. Pei. *Design and fabrication of conformal cooling channels in molds: Review and progress updates*, International Journal of Heat and Mass Transfer 171 (2021) 121082.
- [11] D. Tomasoni, S. Colosio, L. Giorleo, E. Ceretti. *Design for additive manufacturing: Thermoforming mold optimization via conformal cooling channel technology*, Procedia Manufacturing 47 (2020) 1117–1122.
- [12] B. B. Kanbur, S. Suping, F. Duan. *Design and optimization of conformal cooling channels for injection molding: A review*, The International Journal of Advanced Manufacturing Technology 106 (7) (2020) 3253–3271.
- [13] G. S. Phull, S. Kumar, R. S. Walia. *Conformal cooling for molds produced by additive manufacturing: A review*, International Journal of Mechanical Engineering and Technology 9 (1) (2018) 1162–1172.
- [14] C. İ. Çalışkan, G. Özer, E. Koç, U. S. Sarıtaş, C. F. Yıldız, Ö. Y. Çiçek. *Efficiency research of conformal channel geometries produced by additive manufacturing in plastic injection mold cores (inserts) used in automotive industry*, 3D Printing and Additive Manufacturing 10 (2) (2023) 213–225.
- [15] D. Li, H. Wang, N. Dai. *A novel design model of flow channel paths for additive manufacturing*, Rapid Prototyping Journal 30 (6) (2024) 1230–1248.
- [16] C. İ. Çalışkan, A. Koca, G. Özer, Ö. Akbal, S. Bakır. *Efficiency comparison of conformal cooling channels produced by additive and subtractive manufacturing in automotive industry plastic injection moulds: A hybrid application*, The International Journal of Advanced Manufacturing Technology 126 (9) (2023) 4419–4437.
- [17] Y. Wang, C. Lee. *Design and optimization of conformal cooling channels for increasing cooling efficiency in injection molding*, Applied Sciences 13 (13) (2023) 7437.
- [18] S. Feng, A. M. Kamat, Y. Pei. *Design and fabrication of conformal cooling channels in molds: Review and progress updates*, International Journal of Heat and Mass Transfer 171 (2021) 121082.
- [19] C. İ. Çalışkan, G. Özer, M. Coşkun, E. Koç. *Investigation of direct metal laser sintering downskin parameters' sagging effect on microchannels*, The International Journal of Advanced Manufacturing Technology 114 (2021) 2567–2575.
- [20] C. Tan, D. Wang, W. Ma, Y. Chen, S. Chen, Y. Yang, K. Zhou. *Design and additive manufacturing of novel conformal cooling molds*, Materials and Design 196 (2020) 109147.
- [21] W. Heogh, S. M. Yeon, D.-S. Kang, S. Park, S. Park, K. Ryu, J. Sun, L. Ji, Y. Son, K. Choi. *The design and additive manufacturing of an eco-friendly mold utilized for high productivity based on conformal cooling optimization*, Materials and Design 222 (2022) 111088.
- [22] T. Bulsiewicz, P. Łapka. *Effects of additive manufacturing on convective heat transfer in 3D-printed micro/mini-channels and fluid passages with micro/mini structures—The review*, International Communications in Heat and Mass Transfer 159 (2024) 108057.

- [23] Y. Zhu, D. Li, C. Zhang, F. Lin, M. Wu, Y. Chen. *Abrasive flow machining of laser powder bed fusion fabricated mini-channels: Modelling and verification*, Journal of Manufacturing Processes 141 (2025) 36–47.
- [24] X. Xu, E. Sachs, S. Allen, M. Cima, *Designing conformal cooling channels for tooling*, in: D.L.Bourell, J.Beaman, R.Crawford, H. L. Marcus, J.W. Barlow (Eds.), International Solid Freeform Fabrication Symposium, Texas, 1998, pp. 131–146.
- [25] Z. Shayfull, S. Sharif, A. M. Zain, M. F. Ghazali, R. M. Saad. *Potential of conformal cooling channels in rapid heat cycle molding: A review*, Advances in Polymer Technology 33 (1) (2014) 21381.
- [26] S. Feng, A. M. Kamat, Y. Pei. *Design and fabrication of conformal cooling channels in molds: Review and progress updates*, International Journal of Heat and Mass Transfer 171 (2021) 121082.
- [27] C. İ. Çalışkan, G. Özer, M. Coşkun, E. Koç. *Investigation of direct metal laser sintering downskin parameters' sagging effect on microchannels*, The International Journal of Advanced Manufacturing Technology 114 (2021) 2567–2575.
- [28] C. İ. Çalışkan, M. Coşkun, G. Özer, E. Koç, T. A. Vurkır, G. Yöndem. *Investigation of manufacturability and efficiency of micro channels with different geometries produced by direct metal laser sintering*, The International Journal of Advanced Manufacturing Technology 117 (11) (2021) 3805–3817.
- [29] Crucible Industrial Design. Crucible, Design Guidelines for DMLS (2014), <https://www.scribd.com/document/506752344/A-M-Guidelines-Metal>, Accessed 05 Mar 2025.
- [30] EOS Electro Optical Systems, Design Rules for DMLS (2004), <https://www.eos.info/content/blog/how-to-create-differently-with-dmls>, Accessed 05 Mar 2025.
- [31] N. Shamsaei, A. Yadollahi, L. Bian, S. M. Thompson. *An overview of direct laser deposition for additive manufacturing; Part II: Mechanical behavior, process parameter optimization and control*, Additive Manufacturing 8 (2015) 12–35.
- [32] EOS GmbH Electro Optical Systems, EOS Aluminium AlSi10Mg Material Data Sheet (2022), https://www.eos.info/var/assets/03_system-related-assets/material-related-contents/metal-materials-and-examples/metal-material-datasheet/aluminium/material_datasheet_eos_aluminium-alsi10mg_en_web.pdf, Accessed 05 Mar 2025.
- [33] EOS GmbH Electro Optical Systems, StainlessSteel 316L Material Data Sheet (2022), https://www.eos.info/var/assets/03_system-related-assets/material-related-contents/metal-materials-and-examples/metal-material-datasheet/stainlesssteel/material_datasheet_eos_stainlesssteel_316l_en_web.pdf, Accessed 05 Mar 2025.
- [34] EOS GmbH Electro Optical Systems, Titanium Ti64 Material Data Sheet (2022) https://www.eos.info/var/assets/03_system-related-assets/material-related-contents/metal-materials-and-examples/metal-material-datasheet/titan/ti64/eos_ti64_9011-0014_9011-0039_m290_mds_06-22_en.pdf, Accessed 05 Mar 2025.